Leaky Wave Radiation from a Periodically Photoexcited Semiconductor Slab Waveguide

A. Alphones, *Member, IEEE,* and M. Tsutsumi

Abstract—**This paper presents investigations on leaky wave antenna that are modeled by periodical illumination of light on a grounded semiconductor slab waveguide using an asymptotic method of singular perturbation procedure based on multiple scales. Analytical results clearly show that the periodical illumination strongly affects the radiation characteristics such as efficiency and the radiation angle. The dominant effects are studied quantitatively and are outlined in the performance diagrams as a function of optically induced plasma density and the grating period. Initial experimental results at Q band using silicon slab guide under an array of 820-nm LED CW excitation are also reported and are in relatively good agreement with the theory.**

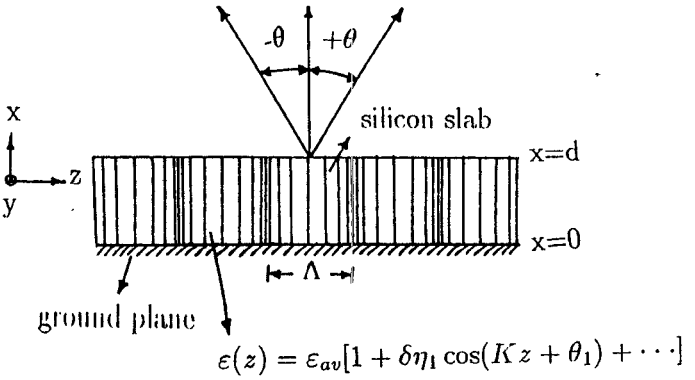

Fig. 1. Permittivity-modulated silicon guide.

I. Introduction

MANY EXCITING developments have been seen in the last decade in the application of optical technology to microwave/millimeter wave devices, circuits, and systems [1]. The optical generation and detection of ultra-short electrical pulses with frequency extending from dc to THz has stimulated a large number of applications in microwave measurement techniques [2]. At the same time, a large amount of effort has been devoted to the optical control of semiconductor devices, both at microwave and millimeter bands [3], [4]. Here, a periodically excited semiconductor waveguide is considered.

A dielectric waveguide with a periodic surface corrugation/permittivity modulation has been shown to hold substantial promise as a leaky wave antenna for millimeter wave applications. Extensive studies have been made on corrugated and index modulated periodic transmission line structures and are reported in the literature [5], [6]. The grating structures used are permanent and normally noncontrollable configurations. However, if the dielectric is of a semiconductor material it is possible to create the grating configuration by means of periodic optical illumination. This correspondingly causes a periodic distribution of photoinduced charge carriers inside the semiconductor material, resulting in a nonpermanent grating configuration. This novelty has been reported in a periodically plasma-induced semiconductor waveguide [7] and also in [8], where a fiber-optically controlled distributed Bragg reflection filter on silicon coplanar waveguide has been investigated. In this paper, a leaky wave antenna that is implemented by periodical illumination of light on a grounded semiconductor slab guide has been studied experimentally using an asymptotic method of singular perturbation procedure based on multiple scales.

Manuscript received January 17, 1995; revised April 1, 1995.

A. Alphones is with the Department of Electronics and Communication Engineering Pondicherry Engineering College, Pondicherry 605 104, India.

M. Tsutsumi is with the Department of Electronics and Information Science, Kyoto Institute of Technology, Kyoto 606, Japan.

IEEE Log Number 9413675.

II. Formulation of the Problem

Fig. 1 shows the theoretical model of the waveguide investigated in this study. It is a semiconductor slab waveguide backed by a conducting ground plane. When the guide is illuminated periodically with optical radiation of photon energy greater than the bandgap energy of the semiconductor, electron-hole plasma is created. The presence of these free carriers results in the modification of the conductive as well as the dielectric properties of the semiconductor material given by Drude-Lorentz theory. The theory predicts that the plasma effects on the dielectric constant will be pronounced at lower frequencies (below optical frequencies). This occurs because at frequencies above the free carrier collision frequency, which characterizes carrier relaxation in the material, the functional dependence of the real and imaginary parts of the dielectric constant are related to the inverse second and third powers of the frequency, respectively [3]

$$\epsilon_p = \epsilon_s - \sum_{i=e,\,h} \frac{\omega_{pi}^2}{\omega^2 + \gamma_i^2}\left(1 + j\frac{\gamma_i}{\omega}\right) = \epsilon_{pr} - j\epsilon_{pi} \qquad (1)$$

where ϵ_s is the dielectric constant of the host lattice, including the contribution of bound charges. γ_i is the collision frequency and is related to relaxation time of the carrier τ_i by $\gamma_i = 1/\tau_i$, ω is the signal frequency, and ω_{pi} is the plasma frequency

given by

$$\omega_{pi}^2 = \frac{n_i e^2}{\epsilon_0 m_i^*}, \qquad i = e, h \tag{2}$$

here n_e is the electron concentration in the conduction band, n_h is the hole concentration in the valence band, m_i^* is the effective mass of electron/hole, e is the electronic charge, and ϵ_0 is the free space permittivity. Typical values used for silicon [3] are $\epsilon_s = 11.8$, $m_e^* = 0.259m_0$, $m_h^* = 0.38m_o$, $\gamma_e = 4.52 \times 10^{12}$/sec., and $\gamma_h = 7.71 \times 10^{12}$/sec.

The transverse magnetic mode is considered here with nonvanishing field components H_y, E_x, and E_z having no variation in the y-direction. By Fourier expansion, a periodically modulated permittivity profile can be expressed as

$$\epsilon(z) = \epsilon_{av}[1 + \delta\eta_1 \cos(Kz + \theta_1) + \delta^2\eta_2 \cos(2Kz + \theta_2) + \cdots] \tag{3}$$

where ϵ_{av} is the average permittivity, η_1 is the amplitude of the fundamental harmonic, δ is the smallness parameter, and K is the grating vector related to the grating period Λ by $(K = 2\pi/\Lambda)$. When the plasma density N_p is modulated periodically by illumination of light, (3) can be rearranged as

$$\epsilon(z) = \epsilon_s \left[1 - \delta \underbrace{\frac{\Delta\epsilon_{pr} + j\Delta\epsilon_{pi}}{\epsilon_s}}_{\eta_1} \cos(Kz + \theta_1) + \cdots\right] \tag{4}$$

and the optically induced modulation index η_1 is deduced, which is complex in nature.

The magnetic field H_y satisfying the differential equation from Maxwell's equations is given by

$$\frac{\partial^2 H_y}{\partial x^2} + \frac{\partial^2 H_y}{\partial z^2} + \omega^2\mu_0\epsilon_0\epsilon_{av}[1 + \delta\eta_1 \cos(Kz + \theta_1) + \delta^2\eta_2 \cos(2Kz + \theta_2)]H_y + \frac{\delta\eta_1 K \sin(Kz + \theta_1) + \delta^2 2\eta_2 K \sin(2Kz + \theta_2)}{1 + \delta\eta_1 \cos(Kz + \theta_1) + \delta^2\eta_2 \cos(2Kz + \theta_2)} \cdot \frac{\partial H_y}{\partial z} = 0. \tag{5}$$

The perturbation is carried up to δ^2 by introducing space scales in the z-direction as $z_0 = z$, $z_2 = \delta^2 z$ with $\partial/\partial z_1 = 0$ and the expansion of H_y is given by

$$H_y(x, z) = H_{y0}(x, z_0, z_2) + \delta H_{y1}(x, z_0, z_2) + \delta^2 H_{y2}(x, z_0, z_2). \tag{6}$$

Substituting (6) into (5), the differential equations for each order are obtained

$$0(\delta^0): \left(\frac{\partial^2}{\partial x^2} + \frac{\partial^2}{\partial z_0^2} + \omega^2\mu_0\epsilon_0\epsilon_{av}\right)H_{y0} = 0 \tag{7}$$

$$0(\delta^1): \left(\frac{\partial^2}{\partial x^2} + \frac{\partial^2}{\partial z_0^2} + \omega^2\mu_0\epsilon_0\epsilon_{av}\right)H_{y1} = -\omega^2\mu_0\epsilon_0\epsilon_{av}\eta_1 \cos(Kz_0 + \theta_1)H_{y0} - \eta_1 K \sin(Kz_0 + \theta_1)\frac{\partial H_{y0}}{\partial z_0} \tag{8}$$

$$0(\delta^2): \left(\frac{\partial^2}{\partial x^2} + \frac{\partial^2}{\partial z_0^2} + \omega^2\mu_0\epsilon_0\epsilon_{av}\right)H_{y2} = -2\frac{\partial^2}{\partial z_0 \partial z_2}H_{y0} - \omega^2\mu_0\epsilon_0\epsilon_{av}\eta_1 \cos(Kz_0 + \theta_1)H_{y1} - \omega^2\mu_0\epsilon_0\epsilon_{av}\eta_2 \cos(2Kz_0 + \theta_2)H_{y0} - \eta_1 K \sin(Kz_0 + \theta_1)\frac{\partial H_{y1}}{\partial z_0} + \frac{\eta_1^2 K}{2} \cdot \sin(2Kz_0 + 2\theta_1)\frac{\partial H_{y0}}{\partial z_0} - 2\eta_2 K \sin(2Kz_0 + \theta_2)\frac{\partial H_{y0}}{\partial z_0}. \tag{9}$$

For each order δ^n, the fields H_y and E_z are continuous at $x = d$. Hence the boundary conditions for each order are given by

$$0(\delta^0): \begin{cases} \frac{\partial}{\partial x}H_{y0f} = 0 & \text{at } x = 0 \\ H_{y0f} = H_{y0c} & \text{at } x = d \\ \frac{\partial}{\partial x}H_{y0f} = \epsilon_{av}\frac{\partial}{\partial x}H_{y0c} & \text{at } x = d \end{cases} \tag{10}$$

$$0(\delta^1): \begin{cases} \frac{\partial}{\partial x}H_{y1f} = 0 & \text{at } x = 0 \\ H_{y1f} = H_{y1c} & \text{at } x = d \\ \frac{\partial}{\partial x}H_{y1f} - \eta_1 \cos(Kz_0 + \theta_1)\cdot \\ \quad \frac{\partial}{\partial x}H_{y0f} = \epsilon_{av}\frac{\partial}{\partial x}H_{y1c} & \text{at } x = d \end{cases} \tag{11}$$

$$0(\delta^2): \begin{cases} \frac{\partial}{\partial x}H_{y2f} = 0 & \text{at } x = 0 \\ H_{y2f} = H_{y2c} & \text{at } x = d \\ \frac{\partial}{\partial x}H_{y2f} - \eta_1 \cos(Kz_0 + \theta_1)\frac{\partial}{\partial x}H_{y1f} \\ \quad -\eta_2 \cos(2Kz_0 + \theta_2)\frac{\partial}{\partial x}H_{y0f} \\ \quad = \epsilon_{av}\frac{\partial}{\partial x}H_{y2c} & \text{at } x = d \end{cases} \tag{12}$$

A. Zeroth-Order Problem

This corresponds to an unperturbed uniform slab waveguide δ^0 problem and the zero-order solutions are sought from (7) and are expressed as

$$H_{y0c} = N_g a_g(z_2)e^{-\alpha_{ci}(x-d)}e^{-j\beta_i z_0} \qquad d \le x < \infty \tag{13}$$

$$H_{y0f} = N_g a_g(z_2)\frac{\cos(k_i x)}{\cos(k_i d)}e^{-j\beta_i z_0} \qquad 0 < x \le d \tag{14}$$

where

$$\alpha_{ci} = \sqrt{\beta^2 - \omega^2\mu_0\epsilon_0} \text{ and } k_i = \sqrt{\omega^2\mu_0\epsilon_0\epsilon_{av} - \beta_i^2}$$

which satisfy

$$\epsilon_{av}\alpha_{ci} = k_i \tan(k_i d). \tag{15}$$

The zero-order field is a slow wave of varying amplitude $a_9(z_2)$ and the normalization constant N_g is chosen by considering the power carrier by the guided wave in the $z-$direction as $|a_g|^2$ over a unit width in the y-direction

$$N_g = \left[\frac{4\omega\epsilon_0\epsilon_{av}\alpha_{ci}k_i^2}{\beta_i[\epsilon_{av}(k_i^2 + \alpha_{ci}^2) + d\alpha_{ci}(\epsilon_{av}^2\alpha_{ci}^2 + k_i^2)]}\right]^{1/2}. \tag{16}$$

B. First-Order Problem

The harmonic variation of the permittivity couples the zeroth-order mode with higher-order Floquet modes, and in the first-order problem many propagating modes must be taken into account, but choosing $n = 1$ the solutions sought from (8) are

$$H_{y1c} = N_r e^{j\theta_1}[a_i e^{jk_{-1c}(x-d)} + b_i e^{-jk_{-1c}(x-d)}]e^{-j(\beta_i - K)z_0} + F_{1c}e^{-\alpha_{1c}(x-d)}e^{-j(\beta_i+K)z_0} \quad (17)$$

$$H_{y1f} = \left[F_{-1f}\frac{\cos(k_{-1f}x)}{\cos(k_{-1f}d)} + G_{-1f}\frac{\sin(k_{-1f}x)}{\sin(k_{-1f}d)} + \frac{\eta_1}{2(2K\beta_i - K^2)}(-\omega^2\mu_0\epsilon_0\epsilon_{av} + K\beta_i) \cdot \frac{\cos(k_i x)}{\cos(k_i d)}N_g a_g e^{j\theta_1}\right]e^{-j(\beta_i - K)z_0} + \left[F_{1f}\frac{\cos(k_{1f}x)}{\cos(k_{1f}d)} + G_{1f}\frac{\sin(k_{1f}x)}{\sin(k_{1f}d)} + \frac{\eta_1}{2(2K\beta_i + K^2)}(\omega^2\mu_0\epsilon_0\epsilon_{av} + K\beta_i) \cdot \frac{\cos(k_i x)}{\cos(k_i d)}N_g a_g e^{-j\theta_1}\right]e^{-j(\beta_i+K)z_0} \quad (18)$$

where

$$k_{-1c} = \sqrt{\omega^2\mu_0\epsilon_0 - (\beta_i - K)^2}$$

$$\alpha_{1c} = \sqrt{(\beta_i + K)^2 - \omega^2\mu_0\epsilon_0}$$

$$k_{-1f} = \sqrt{\omega^2\mu_0\epsilon_0\epsilon_{av} - (\beta_i - K)^2}$$

$$k_{1f} = \sqrt{\omega^2\mu_0\epsilon_0\epsilon_{av} - (\beta_i + K)^2}.$$

The first-order solutions contain $(\beta_i - K)$ and $(\beta_i + K)$ terms, which are the wavenumbers in the z-direction. In the presence of a periodic perturbation, at least one of the scattered Floquet modes must be a fast wave to obtain leaky wave phenomena. This can be accomplished by choosing K such that only $(\beta_i - K)$ lies in the fast wave region $0 < (\beta_i - K) < \omega\sqrt{\epsilon_0}$ and all other Floquet modes as slow waves.

The normalization factor N_r is evaluated by considering the power flow in the $-x$ and $+x$ directions as incident $|a_i|^2$ and radiated $|b_i|^2$ powers, respectively

$$N_r = \left[\frac{2\omega}{k_{-1c}}\right]^{1/2}. \quad (19)$$

The application of boundary conditions of (11) at $x = 0$ yields

$$G_{-1f} = G_{1f} = 0 \quad (20)$$

and at $x = d$, F_{-1f} and F_{1f} are also obtained. Elimination of these amplitude constants lead to a canonical equation relating incident a_i, guided a_g, and radiated b_i waves

$$b_i = C_{rg}a_g + C_{rr}a_i \quad (21)$$

where C_{rg} is the coupling coefficient and C_{rr} is the reflection coefficient, expressed as

$$C_{rg} = \frac{N_g\eta_1}{2N_r(2K\beta_i - K^2)}[k_{-1f}\tan(k_{-1f}d) - j\epsilon_{av}k_{-1c})]^{-1} \cdot \{\omega^2\mu_0\epsilon_0\epsilon_{av}[k_i\tan(k_i d) - k_{-1f}\tan(k_{-1f}d)] - K[k_i\tan(k_i d)(K - \beta_i) - \beta_i k_{-1f}\tan(k_{-1f}d]\} \quad (22)$$

and

$$C_{rr} = -\frac{k_{-1f}\tan(k_{-1f}d) + j\epsilon_{av}k_{-1c}}{k_{-1f}\tan(k_{-1f}d) - j\epsilon_{av}k_{-1c}}. \quad (23)$$

C. Second-Order Problem

The treatment of second-order analysis is necessary for the determination of the guided-mode amplitude and the phase change of the periodic structure. The inhomogeneous second-order problem has a solution if a certain solvability condition is satisfied. The solvability condition is the amplitude transport equation governing the nature of interactions between the zero, first, and second-order fields. The solution for the second-order field is sought in the form

$$H_{y2f} = \Phi_f(x)e^{-j\beta_i z_0} \quad (24)$$

$$H_{y2c} = \Phi_c(x)e^{-j\beta_i z_0}. \quad (25)$$

Substituting these equations into (9) and solving the differential equations for $\Phi_f(x)$ and $\Phi_c(x)$, the solutions obtained are

$$\Phi_c(x) = A_1 e^{-\alpha_{ci}(x-d)} - \frac{j\beta_i x}{\alpha_{ci}}N_g\frac{da_g}{dz_2}e^{-\alpha_{ci}(x-d)} \quad (26)$$

and

$$\Phi_f(x) = B_1\frac{\cos(k_i x)}{\cos(k_i d)} + C_1\frac{\sin(k_i x)}{\sin(k_i d)} + \frac{j\beta_i N_g}{k_i}\frac{x\sin(k_i x)}{\cos(k_i d)} \cdot \frac{da_g}{dz_2}\frac{-\omega^2\mu_0\epsilon_0\epsilon_{av}\eta_1}{2}\left\{\frac{F_{-1f}e^{-j\theta_1}}{(K^2 - 2K\beta_i)} \cdot \frac{\cos(k_{-1f}x)}{\cos(k_{-1f}d)} + \frac{F_{1f}e^{j\theta_1}}{(K^2 + 2K\beta_i)}\frac{\cos(k_{1f}x)}{\cos(k_{1f}d)} + \frac{N_g a_g\eta_1(\beta_i^2 - k_i^2)}{2k_i(4\beta_i^2 - K^2)}\frac{x\sin(k_i x)}{\cos(k_i d)}\right\} + \frac{(K - \beta_i)\eta_1}{2(K - 2\beta_i)}\frac{\cos(k_{-1f}x)}{\cos(k_{-1f}d)}F_{-1f}e^{-j\theta_1} + \frac{(K + \beta_i)\eta_1}{2(K + 2\beta_i)}\frac{\cos(k_{1f}x)}{\cos(k_{1f}d)}F_{1f}e^{j\theta_1} + \frac{\eta_1^2 N_g a_g}{4k_i(4\beta_i^2 - K^2)}(2\beta_i^2\omega^2\mu_0\epsilon_0\epsilon_{av} - K^2k_i^2)b \cdot x\frac{\sin(k_i x)}{\cos(k_i d)}. \quad (27)$$

Application of the boundary conditions of (12) at $x = 0$ yields $C_1 = 0$ and at $x = d$, followed by the elimination of the arbitrary constants, leads to a solvability condition given by

$$\frac{da_g}{dz_2} = C_{gg}a_g + C_{gr}a_i \quad (28)$$

where

$$C_{gr} = \frac{k_i^2 \epsilon_{av} \alpha_{ci} k_{-1c} \eta_1 N_r}{\beta_i D(2K\beta_i - K^2) N_y} \cdot [k_{-1f} \tan(k_{-1f} d) - j\epsilon_{av} k_{-1c}]^{-1} \cdot \{\epsilon_{av}\alpha_{ci}(k_{-1f}^2 + \beta_i^2 - K\beta_i) - k_{-1f} \tan(k_{-1f} d)[k_i^2 + \beta_i(\beta_i - K)]\} \quad (29)$$

and

$$C_{gg} = \frac{j k_i^2 \epsilon_{av} \alpha_{ci} \eta_1^2}{4\beta_i D}(P_1 + P_2 + P_3) \quad (30)$$

where (see (31) and (32), shown at the bottom of the page) and

$$P_3 = \frac{\alpha_{ci} d \tan(k_i d)}{k_i(K^2 - 4\beta_i^2)}[k_i^2 K^2 - (\beta_i^2 + k_i^2)^2] - 2\alpha_{ci}\frac{\beta_i^2 - k_i^2}{K^2 - 4\beta_i^2} - \frac{(dk_i + \tan(k_i d)}{k_i \epsilon_{av}(K^2 - 4\beta_i^2)} \cdot [(\beta_i^2 + k_i^2)^2 - K^2 k_i^2] \quad (33)$$

and

$$D = \epsilon_{av}(k_i^2 + \alpha_{ci}^2) + d\alpha_{ci}(\epsilon_{av}^2 \alpha_{ci}^2 + k_i^2). \quad (34)$$

Equations (21) and (28) constitute a pair of canonical equations relating guided wave, an incident wave, and a radiated wave. C_{gg} is called the extinction coefficient and its real part gives the leakage coefficient C_{ggr}. The imaginary part of the extinction coefficient C_{ggi} determines the exact radiation angle for optimum radiation efficiency.

In a leaky wave antenna problem, the incident wave a_i is not considered, since it is based on the scattering of guided waves into a radiated wave due to the presence of a nonuniformity along the waveguide and hence (21) reduces to

$$b_i = C_{rg} a_g. \quad (35)$$

In a finite length L of the permittivity modulated structure, the radiation efficiency Q_0 is defined as the ratio of the total power radiated from the modulated region to the guided wave power incident at $z_2 = 0$ and is expressed by

$$Q_0 = \frac{\int_0^L |b_i|^2 dz_2}{|a_g|^2_{z_2=0}} = 1 - e^{2C_{ggr}L} \quad (36)$$

and the radiation angle is given by

$$\theta_r = \tan^{-1}\left[\frac{k_{-1c}}{(\beta_i - K + C_{ggi})}\right]. \quad (37)$$

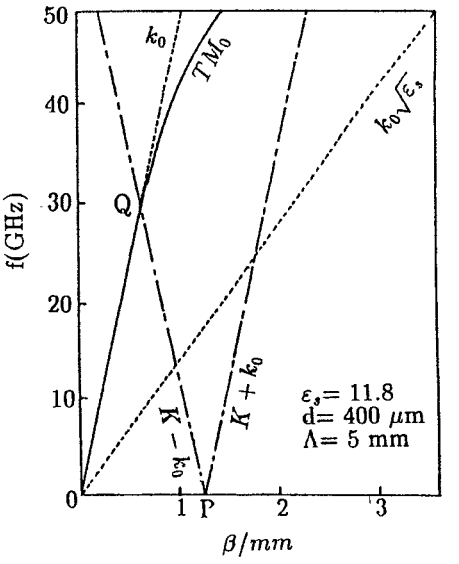

Fig. 2. Dispersion diagram of grounded silicon guide.

III. Numerical Results

Fig. 2 shows a dispersion diagram of the fundamental TM mode supported by the unperturbed silicon waveguide without periodic light illumination. It is assumed that the relative permittivity of the silicon is 11.8 and the thickness of the guide is 400 μm. The phase constant of the fundamental space harmonic when the periodic permittivity modulation applied is assumed to be same as the unperturbed phase constant. In Fig. 2, the regions where the guided waves are purely bounded and where waves become leaky are shown by long dashed lines for the period of 5 mm. At the frequency operating outside the triangle OPQ, leaky wave phenomena occur.

The real and imaginary parts of extinction coefficient C_{ggr} and C_{ggi} are numerically evaluated as a function of frequency for the plasma density of $N_p = 10^{20}/m^3$, i.e., η_1 is approximately 10%, are shown in Fig. 3. Next, for a fixed frequency of 46 GHz, the radiation efficiency and the angle of radiation are estimated as a function of plasma density and are shown in Fig. 4. As the plasma density increases, the radiation efficiency also increases and at the plasma density of $10^{20}/\mathrm{m}^3$, 25% radiation efficiency is obtained. However, even if the modulation index corresponding to the above plasma density is around 10%, the radiation angle does not vary much with the plasma density. Fig. 5 shows the radiation efficiency and the angle of radiation as a frequency dependence for the plasma

$$P_1 = \left[\frac{\epsilon_{av}\alpha_{ci}(k_{-1f}^2 + \beta_i^2 - K\beta_i) - k_{-1f}\tan(k_{-1f}d)(k_i^2 - \beta_i(K - \beta_i))}{(k_{-1f}\tan(k_{-1f}d) - j\epsilon_{av}k_{-1c})(K^2 - 2K\beta_i)^2}\right] \cdot [\alpha_{ci}(k_{-1f}^2 + \beta_i^2 - K\beta_i) - jk_{-1c}(k_i^2 - \beta_i(K - \beta_i))] \quad (31)$$

$$P_2 = \left[\frac{\epsilon_{av}\alpha_{ci}(k_{1f}^2 + \beta_i^2 + K\beta_i) - k_{1f}\tan(k_{1f}d)(k_i^2 + \beta_i(K + \beta_i))}{(k_{1f}\tan(k_{1f}d) - \epsilon_{av}\alpha_{1c})(K^2 + 2K\beta_i)^2}\right] \cdot \{\alpha_{ci}(k_{1f}^2 + \beta_i^2 + K\beta_i) - \alpha_{1c}[k_i^2 + \beta_i(K - \beta_i)]\} \quad (32)$$

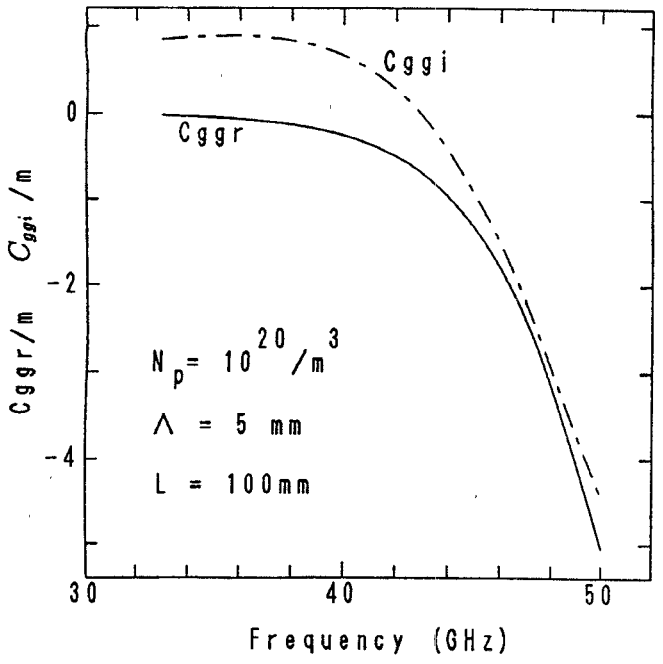

Fig. 3. Variation of C_{ggr} and C_{ggi} with frequency.

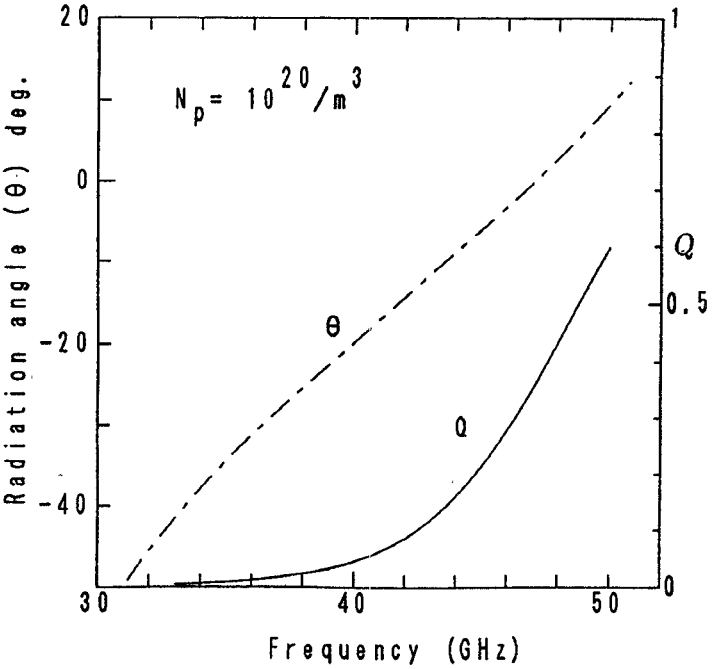

Fig. 5. Frequency dependence of radiation efficiency and the angle of radiation.

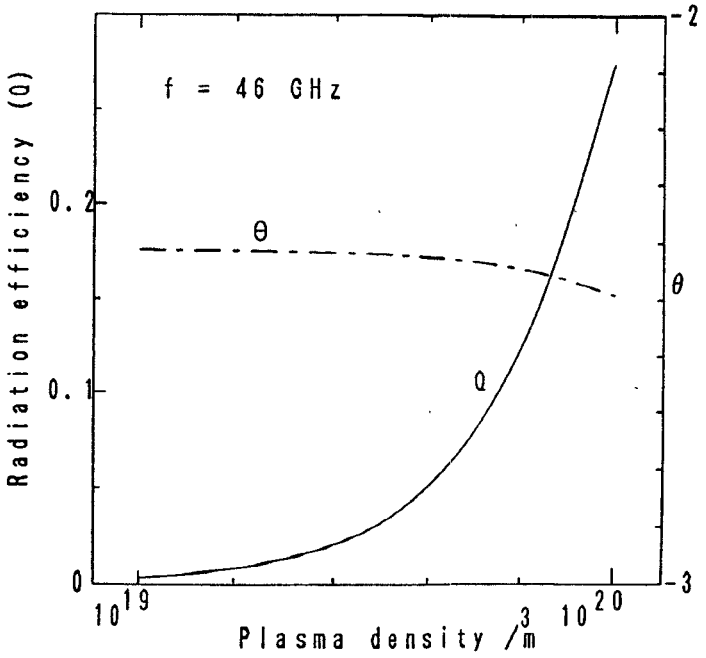

Fig. 4. Radiation efficiency and the angle of radiation as a function of plasma density.

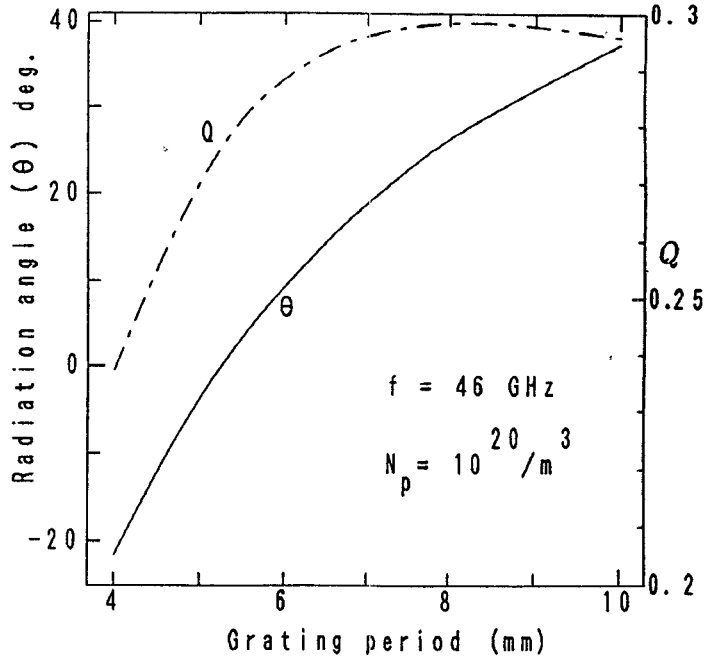

Fig. 6. Radiation angle and radiation efficiency as a function of grating period.

density of $10^{20}/\mathrm{m}^3$. It is clear from this figure that the beam can be steered by the operating frequency and the scanning range is found to be −48–12° at Q band (33–50 GHz). By changing the modulation period the frequency radiating toward broadside ($\theta = 0$) and endfire ($\theta = 10°$) are calculated and plotted in Fig. 6. It is found that by changing the periodicity of illumination pattern the radiation angle could be varied. In other words, it is equivalent to a change of radiation frequency for a fixed radiation angle at 10°. Also at a frequency of 46 GHz and for the plasma density of $10^{20}/\mathrm{m}^3$, the radiation angle and the radiation efficiency have been numerically estimated as a function of the modulation period and are shown in Fig. 7. This shows that the radiation angle can be controlled optically with high efficiency if the periodicity of optical illumination is changed. The radiation pattern has been numerically estimated from

$$R(\theta) = \left| \frac{\sin \frac{N\Psi}{2}}{N \sin \frac{\Psi}{2}} \right|^2 \tag{38}$$

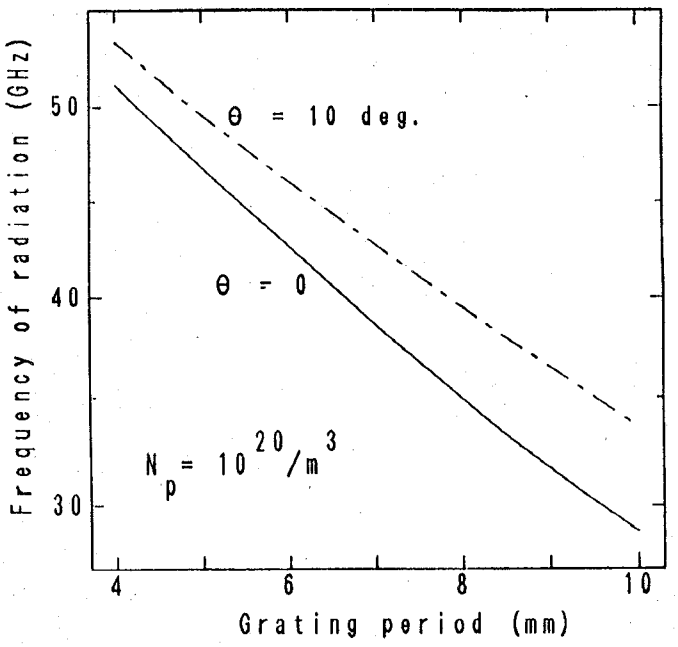

Fig. 7. Radiation frequency versus grating period.

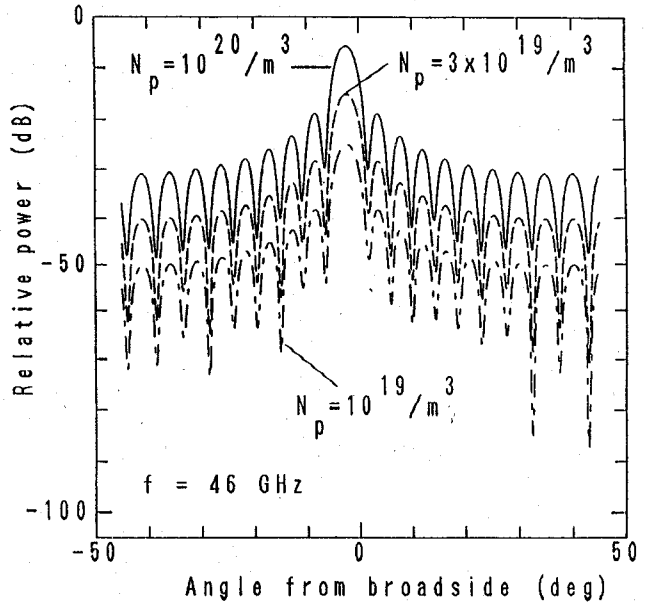

Fig. 8. Theoretically predicted radiation pattern for three different plasma densities.

where

$$\Psi = k_0 \Lambda \sin\theta - \beta_i \Lambda \tag{39}$$

where N is the number of periodic cells. Λ is the grating period, and θ is the angle of radiation from broadside. Fig. 8 depicts the effect of plasma density on radiation pattern shown for three plasma densities. As the plasma density is increased, the radiated power becomes significant, and for the plasma density of $10^{20}/\mathrm{m}^3$ the relative radiated power at 46 GHz is -5 dB with the first side lobe level of 20 dB down. These numerical estimations show that the periodic illumination of semiconductor guide exhibit interesting performance of leaky wave antenna.

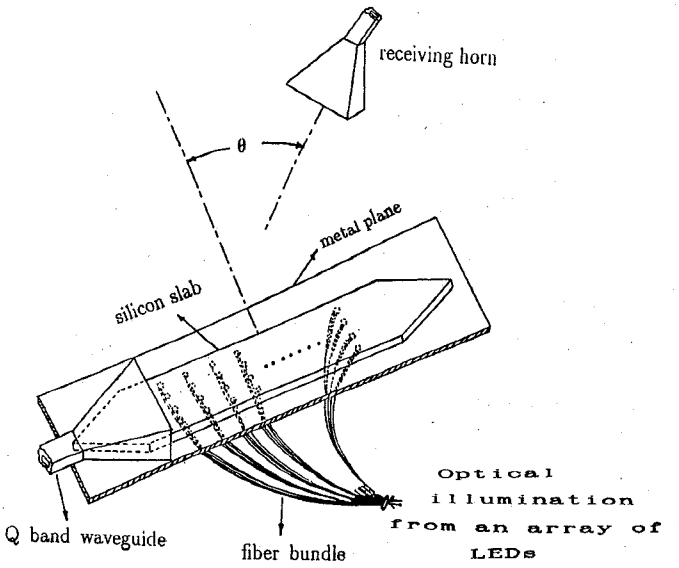

Fig. 9. Schematic diagram of the test section to observe leaky wave radiation.

IV. Experimental Observations

To investigate the optical control experimentally, measurements have been carried out at Q band. High resistivity silicon slab having a resistivity of 5000 Ω.cm is used in this experiment. Slab width is 10 mm and 400 μm thick. To enhance the launching efficiency, the silicon guide has a tapered transition at the input end that is placed into the open end of the rectangular waveguide covered with horn. The far end of the antenna is also tapered and covered with an absorber material for reduction of unwanted reflections. The schematic diagram of the test section is shown in Fig. 9. In the ground plane, small holes are made to place the fiber underneath the slab. In the transverse direction of the ground plane, four equidistant holes of diameter 1.1 mm are made. Twenty such arrays are made with a period of 5 mm in the longitudinal direction. Since these holes are arranged in a periodic manner, the periodic illumination pattern can be achieved by means of the fiber bundle array distribution, which creates a periodically index modulated structure as given by (3). In each hole three equally sized fibers of diameter 0.5 mm are positioned and as a whole 240 fibers are used to illuminate from the underside of the slab guide. A circular array of 5 LED's operating at a wavelength of 820 nm are used to illuminate the structure. To detect the leaky wave signal, a standard horn is fixed far from the center of the slab, which is rotatable 90° toward the backfire and endfire directions from the broadside. With this arrangement the radiation pattern with illumination have been measured and are compared with the theoretically estimated pattern. The experimentally observed pattern closely agrees with theoretical predictions. The asymmetric characteristic of the experimentally observed pattern might be due to the periodic holes made on the ground plane. It is found that the induced plasma by optical

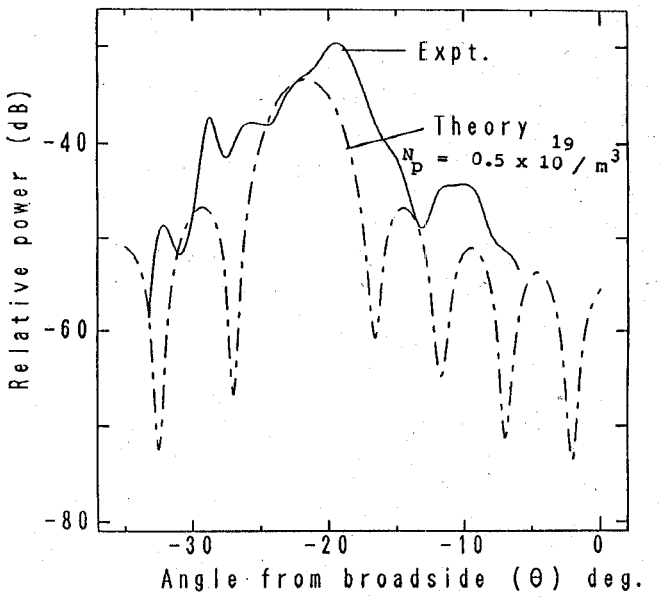

Fig. 10. Experimentaly observed radiation pattern.

illumination might be on the order of $10^{19}/m^3$. Using high-power LED's, the performance of radiation efficiency can be further improved. In this arrangement, to have the flexibility of changing the periodicity, continuous array of LED's and driving the LED's with appropriate period, a variable grating period can be achieved.

V. Conclusion

The leaky wave characteristics on a grounded silicon slab with periodical illumination are analyzed rigorously by a singular perturbation method based on multiple scales. The radiation characteristics such as leakage coefficient and the radiation pattern are numerically estimated. Also, the experiment has been carried out at Q band using a periodic fiber bundle array illuminated by an array of LED's. It is found that the periodic holes in the ground plane used for the fiber array positioning dominate the loss of signal. Using appropriate low loss fibers and by employing better illumination arrangements, the effectiveness of controlling the leaky wave radiation can be successfully improved.

References

[1] R. Simons, *Optical Control of Microwave Devices.* Boston: Artech House, 1990.
[2] K. J. Weingarten, M. J. N. Rodwell, and D. M. Bloom, "Picosecond optical sampling of GaAs integrated circuits," *IEEE J. Quantum Electron.*, vol. 24, pp. 198–220, 1988.
[3] C. H. Lee, "Picosecond optics and microwave technology," *IEEE Trans. Microwave Theory Tech.*, vol. 38, pp. 596–607, 1990.
[4] M. Tsutsumi and A. Alphones, "Optical control of millimeter waves in the semiconductor waveguide," *IEICE Trans. Electron.*, vol. E76-C, pp. 175–182, Feb. 1993.
[5] S. R. Seshadri, "Coupling of guided modes in thin films with surface corrugation," *J. Appl. Phys.*, vol. 63, pp. R115–146, 1988.
[6] S. T. Peng, "Rigorous formulation of scattering and guidance by dielectric grating waveguides: General case of oblique incidence," *J. Opt. Soc. Am. A.*, vol. 6, pp. 1869–1883, 1989.
[7] M. Matsumoto, M. Tsutsumi, and N. Kumagai, "Radiation of millimeter waves from a dielectric waveguide with a light induced grating layer," *IEEE Trans. Microwave Theory Tech.*, vol. MTT-35, pp. 1033–1042, 1987.
[8] W. Platte, "LED induced distributed Bragg reflection microwave filter with fiber-optically controlled change of center frequency via photo conductivity gratings," *IEEE Trans. Microwave Theory Tech.*, vol. 39, pp. 359–363, 1991.

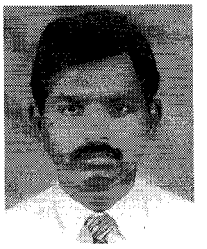

A. Alphones (S'82–M'89) was born on May 2, 1959, in Coimbatore, India. He received the B.Sc. degree in applied sciences from the University of Madras in 1979, B. Tech. (Hons.) degree in electronics from Madras Institute of Technology in 1982, and M. Tech. degree in microwave and optical communication engineering from Indian Institute of Technology, Kharagpur, in 1984. He received the Ph.D. degree from Kyoto Institute of Technology, Japan, in 1992.

From 1984 to 1988, he was with Radar and Communication Centre, IIT Kharagpur, as a Research Fellow and was involved in the research projects. At present, he is working as Assistant Professor in the Department of Electronics and Communication Engineering, Pondicherry Engineering College, India. His current interests are electromagnetics of optical fibers, numerical modeling of microwave and millimeter wave devices and optical-microwave interaction.

Dr. Alphones received the IEEE AES/COM Chapter India award in 1986 in the area of communications. He is a Fellow of Optical Society of India, and member of the Institution of Electronics and Telecommunication Engineers (India).

M. Tsutsumi, photograph and biography not available at the time of publication.